SHORT COMMUNICATION

Open Access

CrossMark

Preclinical evaluation of [68Ga]NOTA-pentixafor for PET imaging of CXCR4 expression in vivo — a comparison to [68Ga]pentixafor

Andreas Poschenrieder[1*] (ID), Margret Schottelius[1], Markus Schwaiger[2] and Hans-Jürgen Wester[1]

Abstract

Background: Due to its overexpression in a variety of tumor types, the chemokine receptor 4 (CXCR4) represents a highly relevant diagnostic and therapeutic target in nuclear oncology. Recently, [68Ga]pentixafor has emerged as an excellent imaging agent for positron emission tomography (PET) of CXCR4 expression in vivo. In this study, the corresponding [68Ga]-1,4,7-triazacyclononane-triacetic acid (NOTA) analog was preclinically evaluated and compared to the 1,4,7,10-tetraazacyclododecane-1,4,7,10-tetraacetic acid (DOTA) parent compound [68Ga]pentixafor.

Methods: NOTA-pentixafor was synthesized by combining solid and solution-phase peptide synthesis. The CXCR4 receptor affinities of [68Ga]pentixafor and [68Ga]NOTA-pentixafor were determined in competitive binding assays using the leukemic CXCR4-expressing Jurkat T-cell line and [125I]FC131 as the radioligand. Internalization and cell efflux assays were performed using CXCR4-transfected Chem-1 cells. Small-animal PET and biodistribution studies were carried out using Daudi-tumor bearing SCID mice.

Results: [68Ga]NOTA-pentixafor showed a 1.4-fold improved affinity towards CXCR4 (IC_{50}). However, internalization efficiency into CXCR4$^+$-Chem-1 cells was substantially decreased compared to [68Ga]pentixafor. Accordingly, small-animal PET imaging and biodistribution studies revealed a 9.5-fold decreased uptake of [68Ga]NOTA-pentixafor in Daudi lymphoma xenografts (1.7 ± 0.4 % vs 16.2 ± 3.8 % ID/g at 90 min p.i.) and higher levels of non-specific accumulation, primarily in the excretory organs such as the liver, intestines, and kidneys (2.3 ± 0.9 % vs 2.0 ± 0.3 % ID/g, 1.9 ± 0.8 % vs 0.7 ± 0.2 % ID/g, and 2.7 ± 1.1 % vs 1.7 ± 0.9 % ID/g, respectively).

Conclusions: Despite enhanced CXCR4-affinity in vitro, the [68Ga]NOTA-analog of pentixafor showed reduced CXCR4 targeting efficiency in vivo. In combination with enhanced background accumulation, this resulted in significantly inferior PET imaging contrast, and thus, [68Ga]NOTA-pentixafor offers no advantages over [68Ga]pentixafor.

Keywords: GPCR, CXCR4, [68Ga]pentixafor, Pentapeptide, NOTA, PET, Radiopharmaceutical, Tracer, Cancer
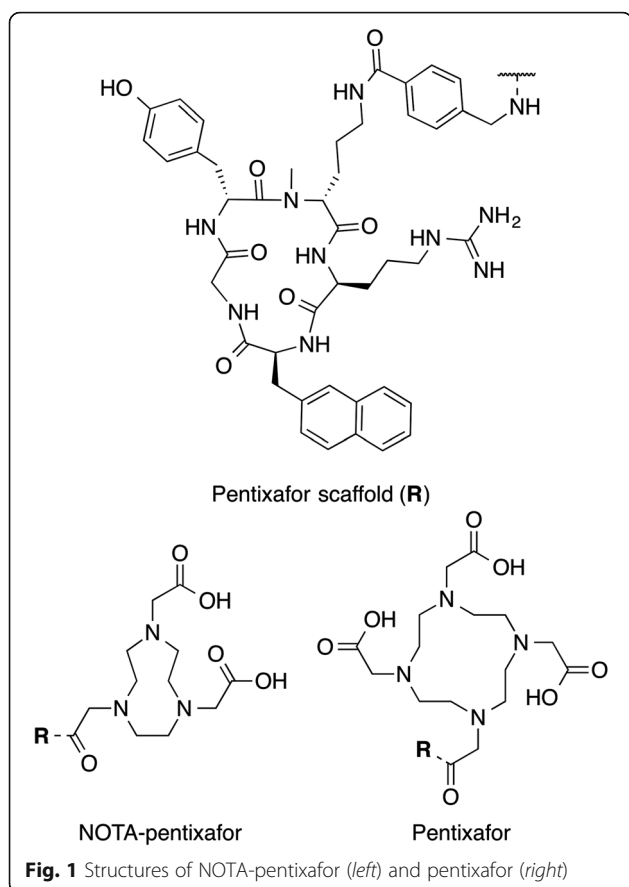
Background

The chemokine receptor 4 (CXCR4) and its only known natural ligand stromal cell derived factor-1 (SDF-1, CXCL12) have gained considerable attention in oncology, in particular its impact on tumor metastasis [1]. Furthermore, overexpression of CXCR4 has been related to poor prognosis and resistance to chemotherapy

[2, 3]. This has led to the development of tools for the non-invasive in vivo quantification of CXCR4 expression in order to improve prognostication and personalized therapy [4]. [68Ga]pentixafor, formerly termed [68Ga]CPCR4.2 (Fig. 1), represents a milestone in the development of CXCR4-targeted positron emission tomography (PET) probes [5, 6], since its pharmacokinetic properties and favorable dosimetry [7] led to a fast transition into first clinical studies, including in vivo quantification of CXCR4 expression in various types of cancers [8–13] and after myocardial infarction

* Correspondence: a.poschenrieder@tum.de
[1]Pharmaceutical Radiochemistry, Technische Universität München, Walther-Meißner-Str.3, 85748 Garching, Germany
Full list of author information is available at the end of the article

Poschenrieder *et al. EJNMMI Research* (2016) 6:70

Page 2 of 5

Fig. 1 Structures of NOTA-pentixafor (*left*) and pentixafor (*right*)

[14–16]. However, triaza-macrocycles like 1,4,7-triazacyclo-nonane-triacetic acid (NOTA) have certain advantages over 1,4,7,10-tetraazacyclododecane-1,4,7,10-tetraacetic acid (DOTA) with respect to chelation of the Ga^{3+} ion [17], e.g. higher thermodynamic stability and kinetic in-ertness [18–20]. Furthermore, [natGa]NOTA-pentixafor had already shown improved affinity towards CXCR4 in a previous study [21]. Therefore, [68Ga]NOTA-pentixa-for was now evaluated preclinically and compared to [68Ga]pentixafor (Fig. 1) with respect to its in vivo CXCR4 targeting ability and overall pharmacokinetic profile.

Methods

General procedures and syntheses of the peptides are described in a recently reported protocol [21]. Determin-ation of tracer lipophilicity [22] and serum stability [23] as well as in vitro studies were performed as recently published [23]. 68Ga-labeling of peptides was performed as described using a fully automated system (Scintomics GmbH) [23]; briefly, the 68Ge/68Ga generator eluate frac-tions (1.25 mL) were reacted with 5 nmol of peptide. The mixture was buffered with 0.6 mL HEPES (pH = 7.4) to a final pH of 3–4 and heated to 95 °C for 5 min. After puri-fication via one Sep-Pak C8 light cartridge, the ethanolic

product fraction was diluted with PBS and used as such for the experiments.

All animal studies were conducted in accordance with the German Animal Welfare Act (Deutsches Tierschutz-gesetz, approval No. 55.2-1-54-2532-71-13). For metabolite analysis, 50 MBq of [68Ga]NOTA-pentixafor in a total volume of 200 µL of PBS was injected into the tail vein of a CB17 SCID mouse; the animal was sacrificed at 1 h p.i. and blood was collected. After sample preparation, as described in [24], the plasma samples were analyzed by reversed phase (RP)-HPLC and eluate fractions were analyzed using a γ-counter.

For PET ($n = 3$) and biodistribution studies ($n = 5$), an average of 15.2 MBq [68Ga]NOTA-pentixafor (100 µL in PBS, 145 pmol, 171 ng) with a specific activity (A_S) of 104 GBq/µmol was injected intravenously into the tail vein of isofluorane anesthesized female Daudi lymphoma-bearing SCID mice. CXCR4 specificity of tumor accu-mulation was demonstrated by co-injection of 2 mg/kg AMD3100 ($n = 3$). After static PET imaging for 15 min (Inveon Siemens µPET scanner), the mice were sacri-ficed (90 min p.i.), and tissues and organs of interest were dissected, weighed, and counted for radioactivity in a γ-counter. The percentage of injected dose per gram of tissue (% ID/g) was calculated; data are shown as mean ± SD.

Results

[68Ga]NOTA-pentixafor was obtained with radiochem-ical yields of 86.6 ± 3.1 % and a maximal specific activity of 128 GBq/µmol. Radiochemical purities were >99 % as confirmed by radio-TLC. As summarized in Table 1, [68Ga]NOTA-pentixafor shows a logP value of −2.4 and is therefore less hydrophilic than its DOTA analog [68Ga]pentixafor (logP = −2.9). CXCR4-affinities of the natGa-complexed peptides and their metal-free precur-sors had already been determined previously [21] and are also shown in Table 1. Both peptides show an in-creased affinity to CXCR4 when metal-labeled, and the natGa-NOTA peptide shows slightly improved CXCR4 affinity compared to the natGa-DOTA parent compound. Compared to [68Ga]pentixafor, total cellular uptake and internalization efficiency of [68Ga]NOTA-pentixafor in CXCR4+ Chem-1 cells are 2.6- and 7.9-fold decreased, re-spectively. While 53.3 % of the total cellular activity was found to be internalized for [68Ga]pentixafor, only 17.5 % of the total cellular activity was internalized in the case of [68Ga]NOTA-pentixafor. Cell efflux studies using [68Ga]NOTA-pentixafor revealed intracellular retention of 44.4 ± 0.04 % and 22.7 ± 0.04 % of the initial cellular activity after 0.5 and 1 h, respectively, indicating limited cellular retention of the tracer.

As already observed for [68Ga]pentixafor (at 30 min p.i.) [5], metabolite analysis of mouse plasma at 60 min p.i. of

Poschenrieder et al. EJNMMI Research (2016) 6:70

Page 3 of 5

Table 1 Comparison of the lipophilicity and the in vitro CXCR4 targeting characteristics of [^{68}Ga]NOTA-pentixafor and [^{68}Ga]pentixafor

Compound	logP	IC$_{50}$ (nM)	Total cellular activity 1 h (%)	Internalized activity 1 h (%)
NOTA-pentixafor	–	253 ± 49	–	–
[^{68}Ga]NOTA-pentixafor	−2.36	17.8 ± 7.7	2.45 ± 0.02	0.43 ± 0.07
Pentixafor	–	102 ± 17	–	–
[^{68}Ga]pentixafor	−2.90	24.8 ± 2.5	6.36 ± 0.46	3.39 ± 0.16

Competitive binding studies (IC$_{50}$) were carried out using Jurkat T cells and [^{125}I]FC131 as the radioligand. For internalization studies, CXCR4$^+$ Chem-1 cells were used

[^{68}Ga]NOTA-pentixafor revealed the complete absence of radiometabolites and thus demonstrates the metabolic stability of the tracer within the observation period.

Comparative biodistribution data for [^{68}Ga]NOTA-pentixafor ($n = 5$) and [^{68}Ga]pentixafor ($n = 6$) in Daudi xenograft bearing CB-17 SCID mice (1.5 h p.i.) are summarized in Table 2. Both tracers show rapid clearance from the circulation and predominantly renal excretion. While retention of [^{68}Ga]pentixafor in the kidneys is low, [^{68}Ga]NOTA-pentixafor shows a 64 % higher kidney uptake. Furthermore, intestinal accumulation

Table 2 Biodistribution data for [^{68}Ga]NOTA-pentixafor and [^{68}Ga]pentixafor in Daudi xenograft bearing CB-17 SCID mice (1.5 h p.i.) and relating tumor-to-organ ratios

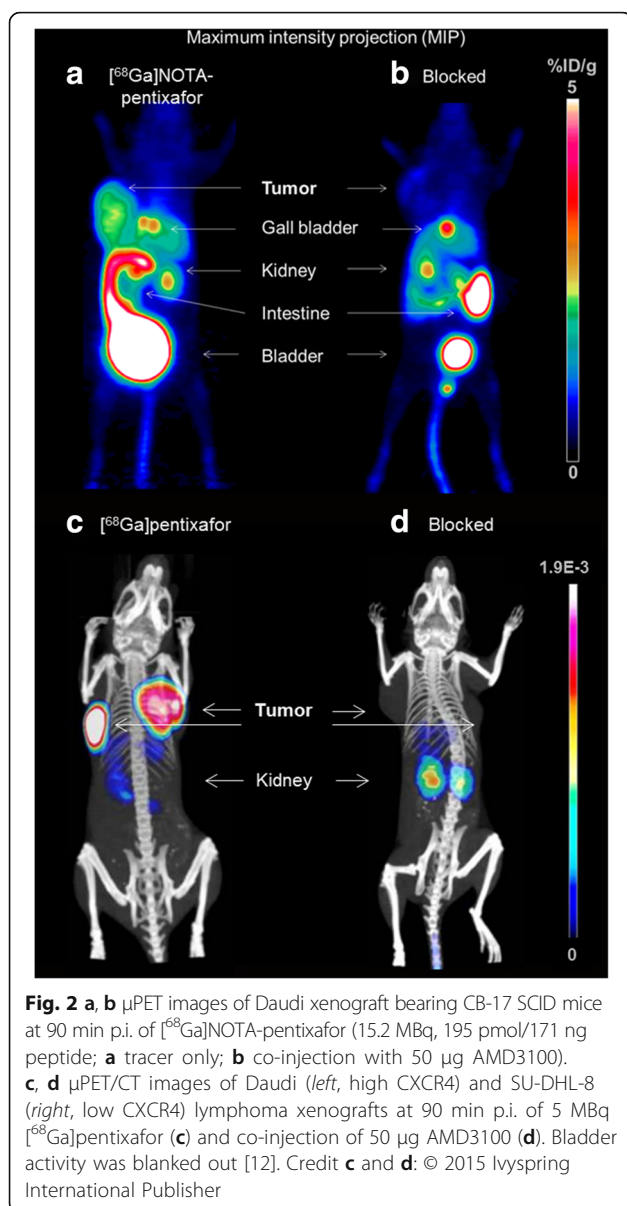| Organ	Tracer		
	[^{68}Ga]NOTA-pentixafor ($n = 5$)	[^{68}Ga]NOTA-pentixafor + AMD3100 ($n = 3$)	[^{68}Ga]pentixafor ($n = 6$)
Blood	0.65 ± 0.41	0.62 ± 0.26	0.97 ± 0.34
Heart	0.34 ± 0.19	0.36 ± 0.14	0.58 ± 0.17
Lung	0.73 ± 0.25	0.95 ± 0.38	1.32 ± 0.29
Liver	2.30 ± 0.88	2.02 ± 0.76	2.05 ± 0.27
Gallbladder	3.61 ± 3.00	5.14 ± 2.24	
Pancreas	0.12 ± 0.05	0.16 ± 0.05	1.06 ± 0.22
Spleen	0.44 ± 0.22	0.54 ± 0.19	0.30 ± 0.10
Kidney	2.71 ± 1.06	3.56 ± 1.03	1.65 ± 0.91
Adrenals	0.52 ± 0.30	0.48 ± 0.15	3.68 ± 0.72
Stomach	0.45 ± 0.21	0.58 ± 0.24	0.48 ± 0.08
Intestine	1.89 ± 0.83	3.97 ± 0.92	0.67 ± 0.21
Muscle	0.13 ± 0.10	0.13 ± 0.05	0.19 ± 0.06
Bone	0.25 ± 0.18	0.16 ± 0.07	n/a
Tumor	1.71 ± 0.40	0.52 ± 0.17	16.2 ± 3.82
Tumor-to-organ ratio			
T/blood	2.64 ± 1.78		16.7 ± 7.05
T/liver	0.74 ± 0.34		7.90 ± 2.13
T/kidney	0.63 ± 0.29		9.81 ± 5.89
T/muscle	13.0 ± 9.86		85.2 ± 33.6

CXCR4 specific tumor accumulation of [^{68}Ga]NOTA-pentixafor was demonstrated by co-injection of 50 μg AMD3100. Data are given in % ID/g tissue and are means ± SD

of [^{68}Ga]NOTA-pentixafor is also 2.8-fold increased compared to the parent compound, most probably due to the increased lipophilicity of the tracer and thus a slightly enhanced hepatobiliary clearance. While the tumor accumulation of [^{68}Ga]pentixafor is higher than activity uptake in all other organs, leading to excellent tumor/background ratios (Table 2), uptake of [^{68}Ga]NOTA-pentixafor in the Daudi xenografts is surprisingly low, albeit CXCR4 specific. This is illustrated by the competition experiment, where co-injection of 50 μg AMD3100 reduced tumor uptake by 70 %. Due to the low absolute tumor uptake of [^{68}Ga]NOTA-pentixafor, however, tumor/organ ratios are <1 for the major excretory organs, suggesting poor imaging contrast.

This was confirmed by small-animal PET imaging studies. Representative PET images of both tracers are shown in Fig. 2. As expected from the biodistribution data, [^{68}Ga]NOTA-pentixafor uptake in the Daudi xenograft was CXCR4 specific (Fig. 2b), and despite low total activity accumulation, tumors were clearly delineated 1.5 h p.i. In contrast to [^{68}Ga]pentixafor, however, which shows virtually no background accumulation except in kidneys [12], [^{68}Ga]NOTA-pentixafor also shows considerable activity accumulation in the gall bladder, intestines, and kidneys.

Discussion

We recently reported the influence of different metal-chelate conjugates of pentixafor on the CXCR4 affinity [21] and found that the NOTA conjugate NOTA-pentixafor (Fig. 1) displayed the highest CXCR4 affinity among various tracers. Because NOTA offers a better suited coordination cavity for Ga^{3+} incorporation and higher thermodynamic stability and kinetic inertness compared to DOTA [18–20], [^{68}Ga]NOTA-pentixafor was now evaluated preclinically and compared to [^{68}Ga]pentixafor (Fig. 1), which is currently entering clinical studies for PET-based quantification of CXCR4 expression in vivo [5, 6, 12]. Surprisingly, despite improving CXCR4 affinity of the ligand, the exchange of DOTA by NOTA had deleterious effects on overall pharmacokinetics, both with respect to CXCR4 targeting efficiency and clearance characteristics. This is mainly attributed to the differences in chelator denticity, overall charge, and

Poschenrieder *et al. EJNMMI Research* (2016) 6:70

Page 4 of 5

Fig. 2 a, b μPET images of Daudi xenograft bearing CB-17 SCID mice at 90 min p.i. of [^{68}Ga]NOTA-pentixafor (15.2 MBq, 195 pmol/171 ng peptide; **a** tracer only; **b** co-injection with 50 μg AMD3100). **c, d** μPET/CT images of Daudi (*left*, high CXCR4) and SU-DHL-8 (*right*, low CXCR4) lymphoma xenografts at 90 min p.i. of 5 MBq [^{68}Ga]pentixafor (**c**) and co-injection of 50 μg AMD3100 (**d**). Bladder activity was blanked out [12]. Credit **c** and **d**: © 2015 Ivyspring International Publisher

resulting changes in the complex geometry, which also affects the lipophilicity (Table 1). The increased logP of [^{68}Ga]NOTA-pentixafor seems to be the main reason for the enhanced background accumulation of the new compound, especially in the gallbladder and intestines. Moreover, the [Ga]NOTA-for-[Ga]DOTA exchange within the pentixafor conjugates alters the overall charge of the chelator moiety from neutral to positive which can also influence the pharmacokinetic profile. The strong dependence of the pharmacokinetics on the chelator and radiometal have also been reported for somatostatin [25, 26] or bombesin-targeting peptides [27]. In contrast, the unexpectedly low tumor accumulation of [^{68}Ga]NOTA-pentixafor in the Daudi xenograft model may be mainly attributed to the substantially decreased internalization

efficiency of [^{68}Ga]NOTA-pentixafor compared to [^{68}Ga]pentixafor, which also seems affected by the structural changes induced by the NOTA-for-DOTA substitution. Such substantial influence of the chelator on the biodistribution has also been shown in human epidermal growth factor receptor type 2 (HER2)-targeting affibodies with DOTA, NOTA, or NODAGA-conjugates [28] as well as other GPCR ligands such as somatostatin receptor-targeting ^{68}Ga-labeled [Tyr^3]octreotide [25].

Conclusion

Despite improved CXCR4 affinity, [^{68}Ga]NOTA-pentixafor showed severely compromised CXCR4 targeting efficiency compared to the parent compound [^{68}Ga]pentixafor, both in vitro and in vivo. Alongside, a substantially decreased uptake in CXCR4-positive lymphoma xenografts, [^{68}Ga]NOTA-pentixafor also shows enhanced accumulation in the excretory organs, leading to low tumor/background ratios and inferior imaging contrast compared to [^{68}Ga]pentixafor. The present data on [^{68}Ga]NOTA-pentixafor underline the strong dependence of the pharmacokinetics of pentixafor-based peptides on the chelator and radiometal and highlight the outstanding characteristics of [^{68}Ga]pentixafor for successful CXCR4 imaging.

Author details
^{1}Pharmaceutical Radiochemistry, Technische Universität München, Walther-Meißner-Str.3, 85748 Garching, Germany. ^{2}Nuklearmedizinische Klinik und Poliklinik, Klinikum rechts der Isar, Technische Universität München, Ismaningerstr. 22, 81675 München, Germany.

Poschenrieder *et al. EJNMMI Research* (2016) 6:70

Page 5 of 5

References

1. Müller A, Homey B, Soto H, Ge N, Catron D, Buchanan ME, et al. Involvement of chemokine receptors in breast cancer metastasis. Nature. 2001;410(6824):50–6.
2. Oda Y, Tateishi N, Matono H, Matsuura S, Yamamaoto H, Tamiya S, et al. Chemokine receptor CXCR4 expression is correlated with VEGF expression and poor survival in soft-tissue sarcoma. Int J Cancer. 2009;124(8):1852–9. doi:10.1002/ijc.24128.
3. Balkwill F. The significance of cancer cell expression of the chemokine receptor CXCR4. Semin Cancer Biol. 2004;14(3):171–9. doi:10.1016/j.semcancer.2003.10.003.
4. George GP, Pisaneschi F, Nguyen QD, Aboagye EO. Positron emission tomographic imaging of CXCR4 in cancer: challenges and promises. Mol Imaging. 2014;13:1–19.
5. Gourni E, Demmer O, Schottelius M, D'Alessandria C, Schulz S, Dijkgraaf I, et al. PET of CXCR4 expression by a (68)Ga-labeled highly specific targeted contrast agent. J Nucl Med. 2011;52(11):1803–10. doi:10.2967/jnumed.111.098798.
6. Demmer O, Gourni E, Schumacher U, Kessler H, Wester HJ. PET imaging of CXCR4 receptors in cancer by a new optimized ligand. Chemmedchem. 2011;6(10):1789–91. doi:10.1002/Cmdc.201100320.
7. Herrmann K, Lapa C, Wester HJ, Schottelius M, Schiepers C, Eberlein U, et al. Biodistribution and radiation dosimetry for the chemokine receptor CXCR4-targeting probe 68Ga-pentixafor. J Nucl Med. 2015;56(3):410–6. doi:10.2967/jnumed.114.151647.
8. Vag T, Gerngross C, Herhaus P, Eiber M, Philipp-Abbrederis K, Graner FP, et al. First experience on chemokine receptor CXCR4 targeted positron emission tomography (PET) imaging in patients with solid cancers. J Nucl Med. 2016;57(5):741–6. doi:10.2967/jnumed.115.161034.
9. Lapa C, Luckerath K, Rudelius M, Schmid JS, Schoene A, Schirbel A, et al. [68Ga]Pentixafor-PET/CT for imaging of chemokine receptor 4 expression in small cell lung cancer - initial experience. Oncotarget. 2016;7(8):9288–95. doi:10.18632/oncotarget.7063.
10. Lapa C, Lückerath K, Kleinlein I, Monoranu CM, Linsenmann T, Kessler AF, et al. 68Ga-Pentixafor-PET/CT for imaging of chemokine receptor 4 expression in glioblastoma. Theranostics. 2016;6(3):428–34. doi:10.7150/thno.13986.
11. Derlin T, Jonigk D, Bauersachs J, Bengel FM. Molecular imaging of chemokine ceceptor CXCR4 in non-small cell lung cancer using 68Ga-Pentixafor PET/CT: comparison with 18F-FDG. Clin Nucl Med. 2016;41(4):e204–5. doi:10.1097/RLU.0000000000001092.
12. Wester HJ, Keller U, Schottelius M, Beer A, Philipp-Abbrederis K, Hoffmann F, et al. Disclosing the CXCR4 expression in lymphoproliferative diseases by targeted molecular imaging. Theranostics. 2015;5(6):618–30. doi:10.7150/thno.11251.
13. Philipp-Abbrederis K, Herrmann K, Knop S, Schottelius M, Eiber M, Luckerath K, et al. In vivo molecular imaging of chemokine receptor CXCR4 expression in patients with advanced multiple myeloma. EMBO Mol Med. 2015;7(4):477–87. doi:10.15252/emmm.201404698.
14. Rischpler C, Nekolla SG, Kossmann H, Dirschinger RJ, Schottelius M, Hyafil F, et al. Upregulated myocardial CXCR4-expression after myocardial infarction assessed by simultaneous GA-68 pentixafor PET/MRI. J Nucl Cardiol. 2016;23(1):131–3. doi:10.1007/s12350-015-0347-5.
15. Thackeray JT, Derlin T, Haghikia A, Napp LC, Wang Y, Ross TL, et al. Molecular imaging of the chemokine receptor CXCR4 after acute myocardial infarction. JACC Cardiovasc Imaging. 2015;8(12):1417–26. doi:10.1016/j.jcmg.2015.09.008.
16. Lapa C, Reiter T, Werner RA, Ertl G, Wester HJ, Buck AK, et al. [(68)Ga]Pentixafor-PET/CT for imaging of chemokine receptor 4 expression after myocardial infarction. JACC Cardiovasc Imaging. 2015;8(12):1466–8. doi:10.1016/j.jcmg.2015.09.007.
17. Viola NA, Rarig RS, Ouellette W, Doyle RP. Synthesis, structure and thermal analysis of the gallium complex of 1,4,7,10-tetraazacyclo-dodecane-N, N ', N '', N '''-tetraacetic acid (DOTA). Polyhedron. 2006;25(18):3457–62. doi:10.1016/j.poly.2006.06.039.
18. Price EW, Orvig C. Matching chelators to radiometals for radiopharmaceuticals. Chem Soc Rev. 2014;43(1):260–90. doi:10.1039/c3cs60304k.
19. Simecek J, Schulz M, Notni J, Plutnar J, Kubicek V, Havlickova J, et al. Complexation of metal ions with TRAP (1,4,7-triazacyclononane phosphinic acid) ligands and 1,4,7-triazacyclononane-1,4,7-triacetic acid: phosphinate-containing ligands as unique chelators for trivalent gallium. Inorg Chem. 2012;51(1):577–90. doi:10.1021/ic202103v.
20. Notni J, Hermann P, Havlickova J, Kotek J, Kubicek V, Plutnar J, et al. A triazacyclononane-based bifunctional phosphinate ligand for the preparation of multimeric Ga-68 tracers for positron emission tomography. Chem-Eur J. 2010;16(24):7174–85. doi:10.1002/chem.200903281.
21. Poschenrieder A, Schottelius M, Schwaiger M, Kessler H, Wester H-J. The influence of different metal-chelate conjugates of pentixafor on the CXCR4 affinity. EJNMMI Res. 2016;6(1):1–8. doi:10.1186/s13550-016-0193-8.
22. Schottelius M, Poethko T, Herz M, Reubi JC, Kessler H, Schwaiger M, et al. First (18)F-labeled tracer suitable for routine clinical imaging of sst receptor-expressing tumors using positron emission tomography. Clin Cancer Res. 2004;10(11):3593–606. doi:10.1158/1078-0432.CCR-03-0359.
23. Poschenrieder A, Osl T, Schottelius M, Hoffmann F, Wirtz M, Schwaiger M, et al. First 18F-labeled pentixafor-based imaging agent for PET imaging of CXCR4 expression in vivo. Tomography. 2016;2(2):85–93. doi:10.18383/j.tom.2016.00130.
24. Weineisen M, Simecek J, Schottelius M, Schwaiger M, Wester HJ. Synthesis and preclinical evaluation of DOTAGAconjugated PSMA ligands for functional imaging and endoradiotherapy of prostate cancer. EJNMMI Res. 2014;4(63):1–15.
25. Lin M, Welch MJ, Lapi SE. Effects of chelator modifications on (68)Ga-labeled [Tyr (3)]octreotide conjugates. Mol Imaging Biol. 2013;15(5):606–13. doi:10.1007/s11307-013-0627-x.
26. Fani M, Del Pozzo L, Abiraj K, Mansi R, Tamma ML, Cescato R, et al. PET of somatostatin receptor-positive tumors using 64Cu- and 68Ga-somatostatin antagonists: the chelate makes the difference. J Nucl Med. 2011;52(7):1110–8. doi:10.2967/jnumed.111.087999.
27. García Garayoa E, Schweinsberg C, Maes V, Brans L, Bläuenstein P, Tourwé DA, et al. Influence of the molecular charge on the biodistribution of bombesin analogues labeled with the [99mTc(CO)3]-core. Bioconjugate Chem. 2008;19(12):2409–16. doi:10.1021/bc800262m.
28. Strand J, Honarvar H, Perols A, Orlova A, Selvaraju RK, Karlstrom AE, et al. Influence of macrocyclic chelators on the targeting properties of (68)Ga-labeled synthetic affibody molecules: comparison with (111)In-labeled counterparts. PLoS ONE. 2013;8(8):e70028. doi:10.1371/journal.pone.0070028.